Journal of Power Sources 196 (2011) 10570–10575

Contents lists available at SciVerse ScienceDirect

Journal of Power Sources

journal homepage: www.elsevier.com/locate/jpowsour

Pt^Ru/C catalysts synthesized by a two-stage polyol reduction process for methanol oxidation reaction

Yuexia Li[a,b], Liping Zheng[a,b], Shijun Liao[a,b], Jianhuang Zeng[a,b,*]

[a] School of Chemistry and Chemical Engineering, South China University of Technology, Guangzhou 510641, China
[b] Guangdong Provincial Key Lab for Fuel Cell Technology & Key Lab of Enhanced Heat Transfer and Energy Conservation, Ministry of Education, China

ARTICLE INFO

Article history:
Received 10 August 2011
Received in revised form 24 August 2011
Accepted 24 August 2011
Available online 31 August 2011

Keywords:
Pt^Ru/C
Methanol oxidation reaction
Catalyst

ABSTRACT

Highly dispersed Ru/C catalysts are prepared using high viscosity glycerol as a reducing agent and are treated in H_2 atmosphere to ensure stability. A Pt^Ru/C catalyst is prepared by an ethylene glycol process based on the pre-formed Ru/C. The catalyst is tested for methanol oxidation reaction at room temperature and is compared with the activity of the as-prepared PtRu/C alloyed catalyst (prepared by co-reduction of Pt and Ru precursors) and commercial PtRu/C from E-TEK. The catalysts are extensively characterized by Transmission electron microscope (TEM), X-ray diffraction (XRD) and X-ray photoelectron spectroscopy (XPS). Electrochemical measurements by cyclic voltammetry (CV) showed consistently high catalytic activities and improved CO resistance for the Pt^Ru/C catalyst.

1. Introduction

The quest for longer battery life has stimulated the fast development of lithium ion battery and low temperature fuel cells. The specific energy density of direct methanol fuel cells (DMFCs) can be 10 times higher than that of lithium ion batteries. At first sight, DMFCs seem to be the most suitable power candidates for portable electronic devices in the replacement of batteries [1]. However, the commercialization of DMFCs largely depends on the developments of key materials such as anode/cathode electrocatalysts and proton exchange membranes [2]. Research on anode electrocatalysts has been mainly devoted to the catalytic activity improvement of Pt based catalyst as well as reduced cost. These include on-going development of different preparative methods [3], investigation on optimized surface structures [4] and particle size [5]. Unfortunately, Pt, as active electrocatalyst, is in demand for many applications in chemical industry, such as catalytic converters for exhaust gas in vehicles, catalysts for petroleum and chemicals processing. Meanwhile, the reservation of Pt in the earth is only hundreds of tons. Pt-only catalysts are therefore very costly. Investigation on non-platinum catalysts or Pt catalysts with lower platinum content without sacrificing catalytic activity is of much significance to promote the commercialization of DMFCs.

Addition to Pt catalysts a second or even a third metal is certainly one of solutions to lower Pt content and the added metals studied so far include Ru, Rh, Sn, W, Se and Mo [6–8], etc. It has been generally accepted that Pt–Ru bimetallic or alloyed catalysts are the most promising anode materials for DMFCs since ruthenium is favorable for removal of the adsorbed CO poisoning intermediates on Pt, which are formed during dehydrogenation steps of methanol oxidation [8–11]. Furthermore, the price of ruthenium is about one-seventh that of platinum, according to current online prices for noble metals.

Another efficient way to decrease the Pt loading, thereby making the most efficient use of noble metal, is to improve dispersions either by using the high surface area supports [5,12,13] or the construction of special structures. These special structures span from alloys [9,11], core–shell [8,10,14,15] and monometallic mixtures [16]. The formation of core–shell structure is probably the most efficient way to improve dispersion [17,18].

To do so, a less noble metal or base metal/metal oxide is usually adopted as core material and Pt is then selectively deposited on the core as a shell to form core–shell construction [17,18]. Alayoglu and Eichhorn reported that Ru@Pt core–shell nanoparticles are far superior to the PtRu alloy and monometallic mixtures in terms of Pt utilization and catalytic activity [16]. Compared with other core materials, the use of Ru core has added advantage since Ru alone can be easily supported on carbon supports with high dispersion. In this work, we used a method to prepare highly active Pt^Ru/C electrocatalyst and systematically evaluated the methanol oxidation performance of the as-prepared PtRu/C alloyed catalysts, Pt^Ru/C and commercially supplied PtRu/C catalysts from E-TEK.

* Corresponding author at: School of Chemistry and Chemical Engineering, South China University of Technology, Guangzhou 510641, China. Tel.: +86 20 87113586; fax: +86 20 87112977.
E-mail address: cejhzeng@scut.edu.cn (J. Zeng).

0378-7753/$ – see front matter © 2011 Elsevier B.V. All rights reserved.
doi:10.1016/j.jpowsour.2011.08.101

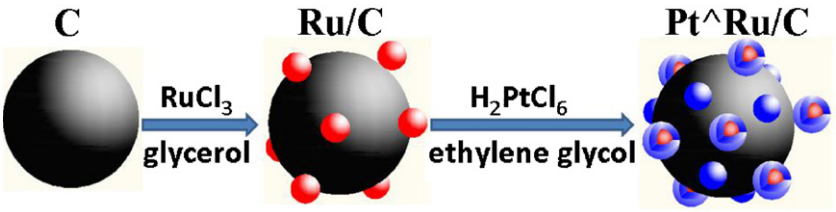

Fig. 1. Illustration for the synthesis of Pt^Ru/C catalyst.

In the preparation of Ru/C, we selected glycerol other than the conventionally used ethylene glycol (EG) as a reducing agent. This step is critical to ensure the formation of highly dispersed Ru/C with small sizes due to the high viscosity of glycerol.

2. Experimental

2.1. Catalyst preparation

Ru/C: carbon-supported Ru was prepared by an organic colloid method in autoclave. 50 mg ruthenium (III) chloride hydrate was dissolved in a mixture of acetone, glycerol and de-ionized water. Sodium citrate (with a molar ratio of 2.5:1 to Ru) was then added with stirring until it was dissolved completely. 200 mg pretreated carbon black (Cabot Corp., S_{BET}: 237 $m^2\,g^{-1}$, denoted as C) were then added to the mixture with stirring, followed by adjustment of the pH to greater than 10 by drop-wise addition of 10 wt.% KOH solution. This mixture was then transferred into an autoclave with a Teflon liner and the temperature was held at 160 °C for 12 h. Ru/C was collected by neutralization with 10 wt.% nitric acid solution, followed by filtration and washing with copious de-ionized water, finally vacuum-dried at 90 °C over night. Then the as-prepared Ru/C was heated for 1 h at 140 °C under flowing H_2 at a flow rate of 50 mL min^{-1}.

Pt^Ru/C catalysts were prepared by microwave-assisted EG process. Calculated amounts of hexachloroplatinic acid ($H_2PtCl_6{\cdot}6H_2O$) and sodium citrate (with a sodium citrate to hexachloroplatinic acid molar ratio of 2.5:1) were dissolved in 20 mL EG under stirring for 30 min. Afterwards, as-modificated Ru/C was added to the mixture and the pH of the solution was adjusted to above 10 by drop-wise addition of 10 wt.% KOH/EG solution. Reduction of Pt was completed by microwave-assisted heating with a microwave power of 400 W for 1 min. It is to be noted that the notation Pt^Ru/C represents the likely structure of isolated Pt and core-shelled Ru@Pt nanoparticles. The total catalyst loading in Pt^Ru/C is kept at 20 wt.% and the atomic ratio of Pt:Ru was held at 1:1.

For a fair comparison, 20 wt.% PtRu/C (1:1) catalysts were prepared by co-reduction of hexachloroplatinic acid and ruthenium chloride following a similar procedure as that of Pt^Ru/C. Commercially available 20 wt.% PtRu/C (1:1), which is sourced from E-TEK, is also included in the work for comparison.

2.2. Catalyst characterization

The surface morphologies of the catalysts were studied via a transmission electron microscope (TEM) (JEOL JEM-2010HR, Japan) operated at 200 kV. X-ray powder diffraction (XRD) analyses were carried out with a Shimadzu XD-3A (Japan), using filtered Cu Kα radiation at 35 kV and 30 mA. The 2θ angular region between 20° and 80° was explored at a scan rate of 4° per min. The X-ray photoelectron spectroscopy (XPS) data were obtained with an Axis Ultra DLD X-ray photoelectron spectrometer (Kratos, USA). The binding energies (BEs) were calibrated using the C 1s peak of graphite at 284.5 eV as the reference.

2.3. Electrochemical measurement

The catalysts were electrochemically evaluated by cyclic voltammetry (CV) using an IM6/IM6e electrochemical work station (Zhaner, Germany) at room temperature. A common three-electrode electrochemical cell was used for the measurements. A platinum wire and a saturated Ag/AgCl electrode were used as counter and reference electrode, respectively. 5 mg catalyst was dispersed ultrasonically in 1 mL Nafion/ethanol (0.25 wt.% Nafion) for 30 min to form homogeneous catalyst ink. The catalyst layer on the 5 mm glassy carbon electrode (served as working electrode) was prepared by pip petting 5 μL ink followed by air drying.

For the electrochemical surface area (ECSA) measurements, 0.5 mol L^{-1} sulfuric acid (H_2SO_4) solutions was used as electrolyte, whereas a 0.5 mol L^{-1} H_2SO_4 plus 0.5 mol L^{-1} methanol (CH_3OH) solution was employed for the evaluation of methanol oxidation activity. For the anodic stripping of CO, 10% CO in Ar was used to saturate the 0.5 mol L^{-1} H_2SO_4 electrolyte for 10 min while the working electrode was held at −0.1 V. The passage of CO was then stopped and the electrolyte was thoroughly purged with high purity N_2 to remove dissolved CO. CO stripping voltammetry then commenced in the potential window of −0.2 V to 0.8 V starting from −0.1 V. The high potential limit was selected at 0.8 V to avoid possible dissolution of ruthenium.

3. Results and discussion

In the present work, Pt^Ru/C catalysts were synthesized by a two-stage route and this is illustrated in Fig. 1. It is understood that ruthenium nanoparticles would selectively supported on carbon

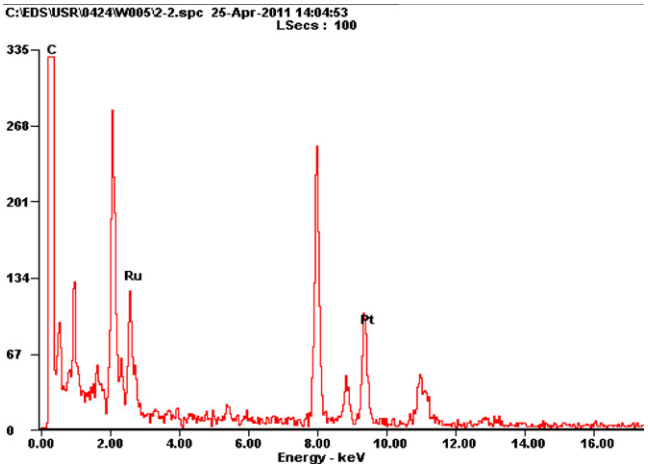

Fig. 2. Energy-dispersive analysis of Pt^Ru/C.

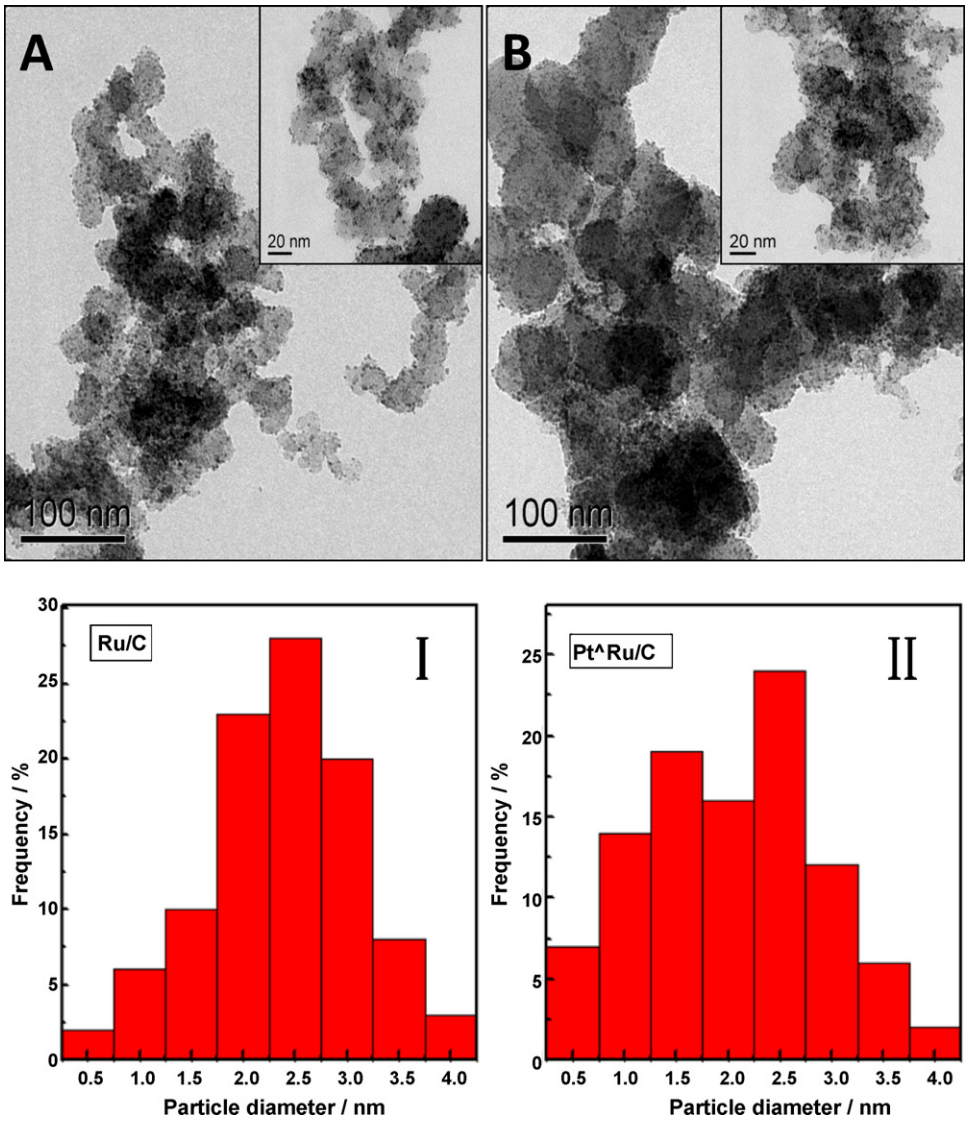

Fig. 3. TEM images of Ru/C (A), Pt^Ru/C (B) and the corresponding particle size distribution of Ru/C (I), Pt^Ru/C (II).

support since the existed carbon supported served as nuclei center for ruthenium nanoparticles to grow. In the synthesis of Ru/C, we used high viscosity glycerol (viscosity at 20 °C: 1412 mPa s) as reducing agent and this procedure is critical for the formation of highly dispersed ruthenium nanoparticles. In comparison, the ruthenium nanoparticles formed in conventionally used ethylene glycol is less dispersed. In glycerol, the mobility of Ru nanoparticles is less flexible than that in ethylene glycol, consequently high dispersion. The dispersion of Ru nanoparticles affects the dispersion of catalyst due to the support effect (supports with high active surface area are generally conducive to the formation of highly dispersed active components). The consequent reduction of Pt would preferably occur on pre-formed Ru/C but the possibility of isolated Pt formation is inevitable. As is shown in Fig. 2, Energy dispersive X-ray (EDX) analyzer attached to a JEOL JEM-2010HR confirmed the existence of Pt and Ru in the catalysts. The PtRu loading of the as-prepared Pt^Ru/C and PtRu/C is 20 wt.% and the atomic ratio of Pt to Ru is 1:1.

Fig. 3A and B shows TEM images of Ru/C and Pt^Ru/C catalyst with different magnifications. It can be seen that the active components (Ru or Pt^Ru) are uniformly dispersed on the carbon support with a narrow size distribution. There are two observable differences between Fig. 3A and B. One is the growth of particle sizes in Fig. 3B relative to A. This feature possibly inferred the formation of Pt on the pre-formed Ru nanoparticles (core–shell structure formation). Another one is the difference in the particle density, which is defined by number of particles per geometric carbon surface area. The particle density of Fig. 3B is higher than that of Fig. 3A, which indicates the possibility of isolated Pt nanoparticles. By counting more than 100 particles in the insert of Fig. 3A and B, the average particle size for Ru/C (I) and Pt^Ru/C (II) is 2.4 nm and 2.0 nm, respectively. It should be noted that the decreased average particle size of Pt^Ru/C is due to the much smaller (relative to Ru nanoparticle) and isolated Pt nanoparticles. From the particle size distribution diagram, it can be seen that Ru/C (I) showed a mono-disperse distribution, whereas Pt^Ru/C (II) showed a bimodal particle size distribution.

Fig. 4 shows the XRD patterns of the catalysts. The graphitic nature of the carbon support in all the catalysts is reflected by the (2 0 0) diffraction peak at 24.8°. Due to the small particle effect, the characteristic Pt–Ru peaks are all poorly resolved. A volume-averaged particle size can be estimated from the Scherrer equation based on the Pt (1 1 0) peak at around 40°, from the line broadening it can be found that the particle sizes decreased in the order: PtRu/C (E-TEK) > as-prepared PtRu/C > Pt^Ru/C. The smaller particle sizes of Pt^Ru/C relative to PtRu/C prepared in our work is possibly due

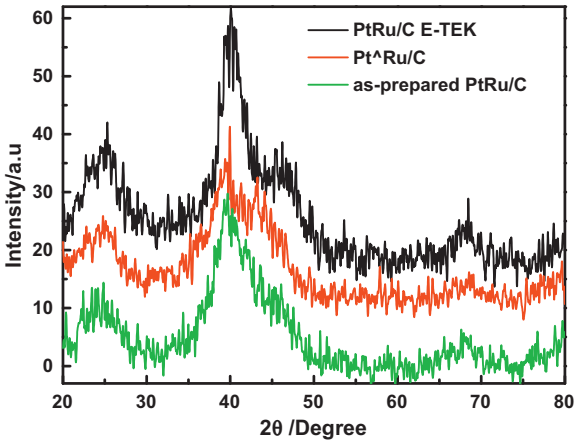

Fig. 4. XRD patterns of Pt^Ru/C, as-prepared PtRu/C and E-TEK PtRu/C catalysts.

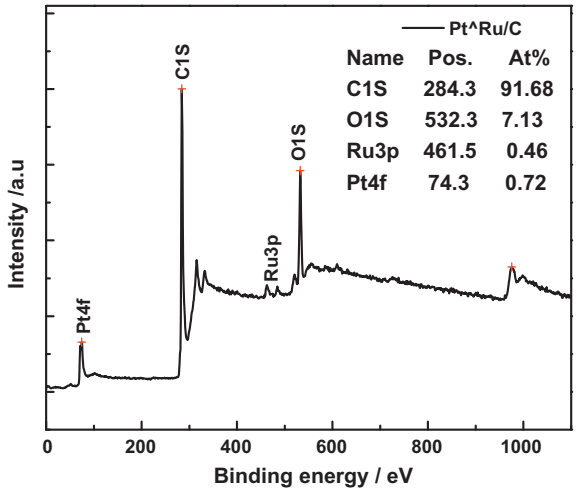

Fig. 5. XPS spectra of Pt^Ru/C catalyst.

to the use of glycerol for the formation of Ru/C. Compared with the conventionally used EG, the viscosity of glycerol is much higher and this is conducive to the formation of very small ruthenium nanoparticles.

It is to be noted that there is a weak but appreciable Ru (1 0 1) diffraction peak at 44.0° for Pt^Ru/C. This character confirmed its preparative procedure since it was synthesized via deposition on pre-formed Ru/C. There is no metallic Ru diffraction peaks in as-prepared PtRu/C and E-TEK PtRu/C and this is an indication of alloyed PtRu as was reported in the literature [15].

XPS was further carried out on the catalysts to obtain information about surface composition and electronic properties. Fig. 5 shows the wide scan XPS spectra of Pt^Ru/C. It can be seen that the detected atomic ratio of Pt to Ru for Pt^Ru/C catalysts was 1.56:1, which was demonstrated that the surface of Pt^Ru/C catalysts enriched by Pt. Since the feeding atomic ratio of Pt^Ru/C is 1:1, the surface-enriched Pt to Ru is a possible indication of Pt covering on pre-formed Ru nanoparticles.

For nano-structured materials, available material characterization techniques are usually insufficient to obtain the exact structure since the material sizes are, sometimes, less than 2 nm. The electrochemical properties of materials are very sensitive to their surface composition and structure and usually used to assist in the identification of material structure [19]. The presence of thin Pt shell over nano-sized Ru particles could be manifested by the electrochemical responses of the core–shell structured particles [20].

Fig. 6 shows the CV results of Pt^Ru/C, as-prepared PtRu/C and E-TEK PtRu/C catalysts in the electrolyte of 0.5 mol L^{-1} H_2SO_4 solution under N_2 atmosphere at room temperature. The current densities of CV plots in this work are both normalized to the geometric surface area and metal loading. The ECSA of the catalysts is calculated according to the literature [5]. The as-prepared PtRu/C and E-TEK PtRu/C showed a dome-shaped hydrogen adsorption/desorption region, which is a characteristics of typical PtRu alloy. In comparison, Pt^Ru/C showed a combined feature of PtRu alloy and Pt alone catalysts: appreciable hydrogen adsorption/desorption peaks can be found in the region of −0.2 V to 0 V and a weak Pt reduction peak can be found at 0.64 V in the backward scan. The double layer of Pt^Ru/C is also thinner than that of E-TEK PtRu/C and as-prepared PtRu/C indicating of less oxides in the catalysts. The electrochemical response of Pt^Ru/C is well reflected by the materials structure since Pt^Ru/C is possibly composed of isolated Pt and Pt-on-Ru core–shell nanoparticles. The ECSA of Pt^Ru/C catalyst is 116.6 m^2 g^{-1} (per unit weight of Pt), which is 2.5 times and 1.2 times than that of E-TEK PtRu/C (46.5 m^2 g^{-1} Pt) and as-prepared PtRu/C (97.2 m^2 g^{-1} Pt) catalysts, respectively.

Fig. 7 shows the methanol oxidation of Pt^Ru/C, as-prepared PtRu/C and E-TEK PtRu/C catalysts in 0.5 mol L^{-1} H_2SO_4 plus 0.5 mol L^{-1} CH_3OH solution at room temperature. The hydrogen adsorption/desorption peak in Fig. 7 differs that in Fig. 6 in the range of −0.2 V to 0 V due to the methanol adsorption on the catalyst surface, consequently suppressed hydrogen adsorption/desorption peak. The peak potential for E-TEK PtRu/C, as-prepared PtRu/C and Pt^Ru/C catalysts is at 0.62 V, 0.63 V and 0.62 V, respectively. The methanol oxidation activity in terms of mass activity can be evaluated by the forward anodic peak current density in the CV of methanol oxidation in Fig. 7b and this is 0.15 A mg^{-1} Pt, 0.23 A mg^{-1} Pt and 0.37 A mg^{-1} Pt for E-TEK PtRu/C, as-prepared PtRu/C and Pt^Ru/C catalysts, respectively. The mass activity of Pt^Ru/C is thus 2.4 times and 1.6 times as high as that of E-TEK PtRu/C and as-prepared PtRu/C catalysts, respectively. Besides of mass activity, the specific activity, which is normalized by the ECSA, reflected the intrinsic activity of the catalysts. The specific activity of the catalysts Pt^Ru/C, as-prepared PtRu/C and E-TEK PtRu/C is calculated to be 9.6, 6.5 and 4.1 mA cm^{-2}, respectively.

Fig. 8 shows the illustrative CO stripping cyclic voltammograms at room temperature in 0.5 mol L^{-1} H_2SO_4 at a scan rate of 20 mV s^{-1} for Pt^Ru/C, as-prepared PtRu/C and E-TEK PtRu/C catalysts. In the potential region between −0.1 V and 0.3 V, hydrogen adsorption was suppressed and CO oxidation commenced at around 0.3 V for all the catalysts. E-TEK PtRu/C and as-prepared PtRu/C displayed only one CO oxidation peak at around 0.38 V, whereas Pt^Ru/C displayed two oxidation peaks, which is at 0.36 V and 0.61 V. This feature is well agreed with the bimodal particle size distribution of Pt^Ru/C in Fig. 3. The peak at around 0.36 V is possibly attributed to the CO oxidation on Pt-on-Ru nanoparticles while the peak at 0.61 V is due to the CO oxidation on isolated Pt nanoparticles.

Pt^Ru/C synthesized in this work is composed of Pt-on-Ru nanoparticles and isolated Pt nanoparticles. This can be well understood by the two stage reduction process where high viscosity glycerol was used to prepare highly dispersed Ru/C and some Pt was selectively formed on pre-formed Ru and some was isolatedly deposited on carbon as Pt alone catalysts. Consequently Pt^Ru/C showed a typical bimodal particle size distribution and partially formed Pt-on-Ru was confirmed by the higher Pt to Ru ratio relative to the feeding 1:1 ratio (XPS). The composite Pt^Ru/C catalyst showed a double CO oxidation peak due to co-existed Pt and Pt-on-Ru nanoparticles.

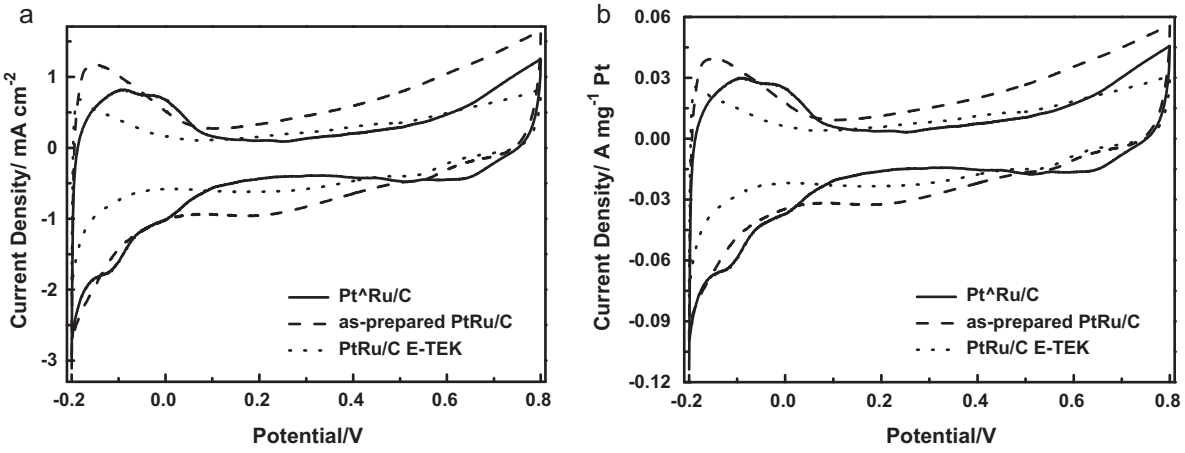

Fig. 6. Cyclic voltammograms of Pt^Ru/C, as-prepared PtRu/C and E-TEK PtRu/C catalysts in 0.5 mol L^{-1} H_2SO_4 solution under N_2 atmosphere at room temperature and at a scan rate of 20 mV s^{-1} (a) normalized to geometric surface area and (b) normalized to the metal loadings.

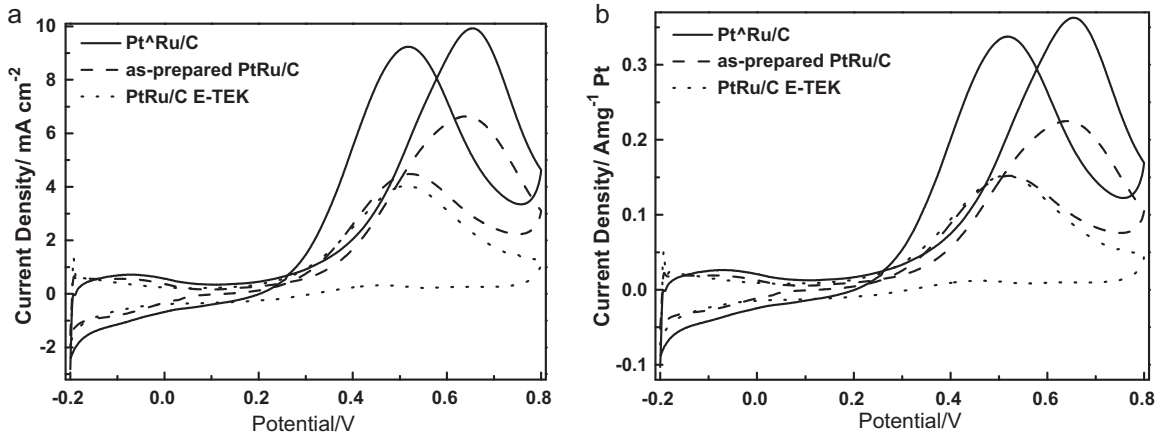

Fig. 7. Cyclic voltammograms of Pt^Ru/C, as-prepared PtRu/C and E-TEK PtRu/C catalysts in 0.5 mol L^{-1} H_2SO_4 plus 0.5 mol L^{-1} CH_3OH solution at room temperature and at a scan rate of 20 mV s^{-1}(a) normalized to geometric surface area and (b) normalized to the metal loadings.

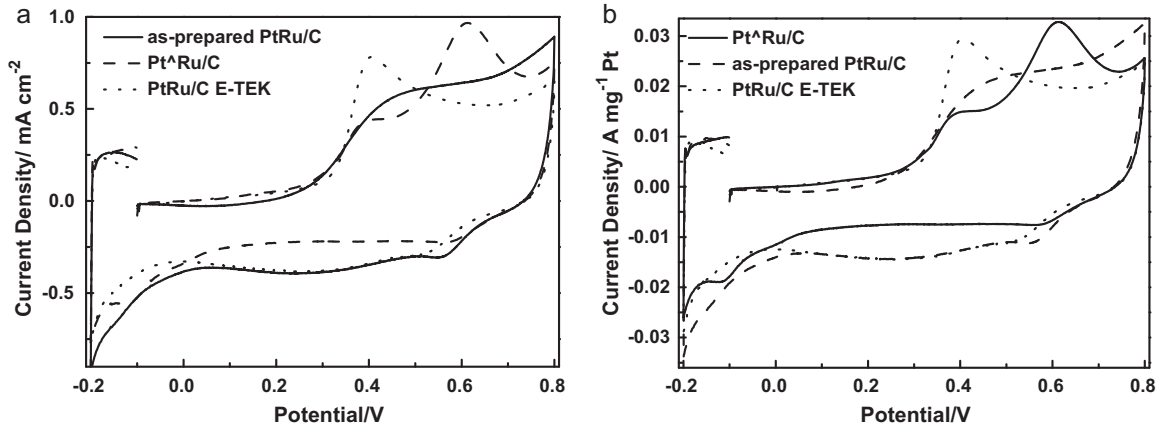

Fig. 8. CO stripping cyclic voltammograms for the catalysts in 0.5 mol L^{-1} H_2SO_4 solution measured at a scan rate of 20 mV s^{-1} at room temperature (a) normalized to geometric surface area and (b) normalized to the metal loadings.

Nevertheless, the Pt^Ru/C catalysts showed enhanced methanol oxidation activity relative to as-prepared PtRu/C and E-TEK PtRu/C possibly due to the improved dispersion and co-existed Pt and Pt-on-Ru nanoparticles.

4. Conclusions

In short summary, a two-stage polyol process was adopted to prepare a more efficient carbon supported Pt^Ru/C catalysts for

methanol oxidation reaction at room temperature. The catalysts are composed of isolated Pt nanoparticles and Pt-on-Ru nanoparticles. The mass-normalized activity for Pt^Ru/C showed 2.4 times and 1.6 times improvement over E-TEK PtRu/C and as-prepared PtRu/C, respectively.

Acknowledgements

The financial support provided by the National Natural Science Foundation of China (Project Nos. 20876062 and 21076089) is gratefully acknowledged.

References

[1] C. Bock, C. Paquet, M. Couillard, G.A. Botton, B.R. MacDougall, J. Am. Chem. Soc. 126 (2004) 8028–8037.
[2] R. Chetty, S. Kundu, W. Xia, M. Bron, W. Schuhmann, V. Chirila, W. Brandl, T. Reinecke, M. Muhler, Electrochim. Acta 54 (2009) 4208–4215.
[3] K. Sasaki, R.R. Adzic, J. Electrochem. Soc. 155 (2008) B180–B186.
[4] B. Yoon, H. Häkkinen, U. Landman, A.S. Wörz, J.M. Antonietti, S. Abbet, K. Judai, U. Heiz, Science 307 (2005) 403–407.
[5] X. Li, W.X. Chen, J. Zhao, W. Xing, Z.D. Xu, Carbon 43 (2005) 2168–2174.
[6] M. Götz, H. Wendt, Electrochim. Acta 43 (1998) 3637–3644.
[7] R.F. Wang, S.J. Liao, H.Y. Liu, H. Meng, J. Power Sources 171 (2007) 471–476.
[8] H.L. Gao, S.J. Liao, J.H. Zeng, Y.C. Xie, J. Power Sources 196 (2011) 54–61.
[9] H.T. Kim, H.I. Joh, S.H. Moon, J. Power Sources 195 (2010) 1352–1358.
[10] S. Alayoglu, A.U. Nilekar, M. Mavrikakis, B. Eichhorn, Nat. Mater. 7 (2008) 333–338.
[11] D. Chu, S. Gilman, J. Electrochem. Soc. 143 (1996) 1685–1690.
[12] C. Paoletti, A. Cemmi, L. Giorgi, R. Giorgi, L. Pilloni, E. Serra, M. Pasquali, J. Power Sources 183 (2008) 84–91.
[13] T. Matsumoto, T. Komatsu, H. Nakano, K. Arai, Y. Nagashima, E. Yoo, T. Yamazaki, M. Kijima, H. Shimizu, Y. Takasawa, J. Nakamura, Catal. Today 90 (2004) 277–281.
[14] X.Z. Fu, Y. Liang, S.P. Chen, J.D. Lin, D.W. Liao, Catal. Commun. 10 (2009) 1893–1897.
[15] R. Wang, H. Li, H. Feng, H. Wang, Z. Lei, J. Power Sources 195 (2010) 1099–1102.
[16] S. Alayoglu, B. Eichhorn, J. Am. Chem. Soc. 130 (2008) 17479–17486.
[17] Z. Liu, G.S. Jackson, B.W. Eichhorn, Angew. Chem. Int. Ed. 122 (2010) 3241–3244.
[18] T. Ghosh, M.B. Vukmirovic, F.J. DiSalvo, R.R. Adzic, J. Am. Chem. Soc. 132 (2009) 906–907.
[19] W. Wang, R. Wang, S. Ji, H. Feng, H. Wang, Z. Lei, J. Power Sources 195 (2010) 3498–3503.
[20] Y. Chen, F. Yang, Y. Dai, W. Wang, S. Chen, J. Phys. Chem. C 112 (2008) 1645–1649.